Desalination and Water Treatment
www.deswater.com
doi: 10.1080/19443994.2014.926648

52 (2014) 5092–5101
July

Taylor & Francis
Taylor & Francis Group

Fouling behavior of urban sewage on binary blend PVDF UF membrane

Xiao-rong Meng[a,*], Hai-zhen Zhang[a], Lei Wang[b], Xu-dong Wang[b], Dan-xi Huang[b]

[a]*School of Science, Xi'an University of Architecture and Technology, Xi'an 710055, China, Tel. +13152171015; emails: mxr5@163.com (X.-r. Meng), zhang120117@126.com (H.-z. Zhang)*
[b]*School of Environmental and Municipal Engineering, Xi'an University of Architecture and Technology, Xi'an 710055, China, emails: wl0178@126.com (L. Wang), xudongw7904@163.com (X.-d. Wang), huangdanxicc@yahoo.com.cn (D.-x. Huang)*

Received 28 November 2012; Accepted 18 May 2014

ABSTRACT

Polyvinylidene fluoride (PVDF) ultrafiltration membranes with better performance were prepared by blending with PVA, polyvinylpyrrolidone, polyethylene glycol, and polymethylmethacrylate through phase inversion via immersion precipitation method. Phase inversion progress of membranes was investigated though light transmittance experiment. Membrane components and morphologies were analyzed by FTIR, scanning electron microscopy, and atomic force microscopy, respectively. Membrane performance was evaluated in terms of pure water permeation, BSA rejection, and water contact angle. Membranes fouling behavior was evaluated according to dynamic fouling resistance analysis, using secondary effluent of urban sewage as separation object. The results showed that PVDF UF membranes with high hydrophilicity, dense surface, and through macrovoids in cross-section had small sewage flux decline and low fouling during filtration, and the main fouling resistance was due to concentration polarization and cake layer resistance, and membrane fouling was reversible. While the UF membranes with porous surface, not through internal macrovoids, and loose sponge-like structure were trend to bring about pore plugging resistance, and membrane fouling was irreversible. The surface roughness had certain influence on the antifouling performance of PVDF UF membranes.

Keywords: PVDF; Blend UF membranes; Secondary effluent of urban sewage; Antifouling

1. Introduction

The urban sewage is potential water resources. Wastewater reclamation is an important means to solve water crisis [1,2]. The performance of polyvinylidene fluoride (PVDF) is excellent and it is widely used in ultrafiltration and microfiltration membrane technology [3,4]. But the strong hydrophobicity of PVDF ultrafiltration membranes makes it easy to be fouled by organics adsorption, thus the performance of membranes deteriorates which severely restricted the progress of ultrafiltration technology in urban sewage reclamation and reuse.

Many studies have been carried out on membranes fouling from the view point of membrane filtration. In which hydrophilic blend modification is the main study direction to improve the antifouling properties

*Corresponding author.

Presented at the Conference on Water Resources and Urbanization Development, 26–27 September 2012, Tianjin, China

of membranes [5,6]. Inorganic nanoparticles, SiO_2, and hydrophilic polymers such as PVA and polyvinylpyrrolidone (PVP) are often used as additives to modify the hydrophilicity of PVDF UF membrane. Performance analysis and research of modified PVDF UF membrane were conducted [7,8], but study results about the antifouling properties of UF membranes were not uniform. Some researchers considered that membranes with high hydrophilicity and low roughness had excellent antifouling; nevertheless, other investigators hold the opinion that there was no clear relationship between membrane hydrophobicity and fouling tendency, and membrane with rough surface had better antifouling. Srivastava et al. [9] prepared series of PVDF–SAN blend membranes for textile wastewater ultrafiltration. The experimental results showed that the hydrophobicity and the antifouling properties of modified PVDF membranes were improved especially for PVDF–SAN UF membrane at 60% SAN content. Zhao et al. [10] prepared modified PVDF–graphene oxide (GO) UF membranes and their study results indicated that PVDF–GO membranes had better antifouling performances due to the improvement of hydrophilicity and the smooth surface of membrane. However, Wang et al. [11] reported that there was no clear relationship between membrane hydrophobicity and fouling tendency. Jeshi and Neville [12] hold the opinion that the decrease in surface roughness can improve antifouling property of RO membranes, but low surface roughness may be disadvantageous to membrane flux. Hashino et al. [13] studied the effect of surface roughness of hollow fiber membranes with gear-shaped structure on membrane fouling. They found that the smooth outer surface of membranes is covered by thick cake layer. While the membrane having the higher projection, the valley was covered by cake layer but the top was clean which is caused by the hydraulic effect, and they showed higher relative permeability. Rahimpour et al. [14] noticed that the feed particles form a layer on the membrane surface with small pores in the top layer. While for the membranes with large pores, the particles enter into the membrane structure and entrap within the pores, causing irreversible fouling. Generally, hydrophilic membranes have better antifouling property, but study results of the influence of roughness on membrane antifouling performance have not been unified. The relationship between roughness and membrane antifouling may depend on the size and properties of foulants particles, the shape and the size of top and valley, and may also depend on the interval between them. The membranes with rougher surface have high flux which may be caused by the increase of membranes effective filtration area due to the high surface roughness.

In this study, membrane fouling behavior of PVDF ultrafiltration membranes, with different structural characteristics and hydrophilicity, which were prepared by blending with hydrophilic modifier PVA, polymethylmethacrylate (PMMA), PVP, and PEG through precipitation phase inversion was investigated by dynamic membrane fouling. The effect of membrane structure and hydrophilicity on membrane and its antifouling properties were evaluated through fouling resistance analysis, aiming to provide basic data for urban sewage ultrafiltration regeneration technology.

2. Experimental

2.1. Materials

PVDF (6020, M_w 573,000 Da, Solef, Belgium), PVA (18-99, Hanxi Sanwei Co. Ltd), N,N-dimethylacetamide (99% purity, FuCheng, Tianjing), BSA (M_w 67,000 Da, ShangHai, Lanji, China), polymethylmethacrylate (PMMA, Sigma), polyvinylpyrrolidone (PVP, K30, Japan), and PEG (20 K, purity, FuCheng, Tianjing).

The secondary effluent was obtained from Bei Shi Qiao sewage purification center in Xi'an. Relative properties of this effluent are described in Table 1. For information of analysis methods of these parameters, see references [15,16]. The sewage water analysis results showed that strong hydrophobic components accounted for 54.1%, the polar hydrophilic components reached 25.9%, while the weak and neutral hydrophilic ingredients were 9.6 and 10.4%, respectively. Thus, the strong hydrophobic and polar hydrophilic components were the main reason that caused fouling during ultrafiltration process.

Table 1
Characteristics of the raw water samples from Bei Shi Qiao sewage purification center

Parameter	Average value
SS (mg L^{-1})	10–20
COD (mg L^{-1})	18–27
TOC (mg L^{-1})	8–10
pH	5–7
Turbidity (NTU)	4–10
Molecular weight distribution (%)	
<30 kDa	64.6
30–50 kDa	19.4
>50 kDa	16

2.2. Preparation of PVDF UF membranes

PVDF UF membranes were prepared by phase inversion via immersion precipitation method [17]. The polymer solution was prepared by adding 3 wt% LiCl, PVA, PVP, PMMA, and PEG in the system of 17 wt% PVDF and 80 wt% DMAc at 60°C, respectively. The homogeneous solution was kept overnight at 60°C after being stirred for 20 h. Then the cast solution was cast onto a glass plate to form liquid film with the thickness of 200 μm. After 5 s exposure in the air, the plate was immersed into a deionized water bath at 40°C. The membranes were rinsed with water and stored in water for at least 48 h before being used. Membrane samples were marked as P, PA, PP, PM, and PG, respectively.

The precipitate speed of membranes was determined by phase separation dynamics tester (XDE-2). The thickness of membranes was 200 μm, the temperature of coagulation bath was set at 45°C, and the data acquisition speed was 50 data per second.

2.3. Membranes characterization

FTIR spectroscopy: FTIR (IR-21, Japan) was used to characterize the composition of PVDF membranes.

Morphology: Scanning electron microscope (SEM, JSM5800, Japan, JEOL) was used to observe the cross-section and surface structure of membranes. The membrane pieces were immersed in liquid nitrogen for freezing. And then the frozen membrane segments were kept in air for drying. The dried samples were gold sputtered for producing electric conductivity. Atomic force microscope (AFM, NanoScope III, America) was employed to analyze the surface roughness of the membranes, and the scan size of the membranes tested was 5 × 5 μm.

Hydrophily: Water contact angle (WCA) was measured using the VCA-Optima (AST products, Inc, MA, USA). About 5 μl of distilled water was dropped on membrane surface from a microsyringe with a stainless steel needle at room temperature (25 ± 1°C). WCA values were obtained for the top surface of each membrane sample and keep the time 30 s.

Structural parameters: Porosity of membrane (ε) was measured by wet and dry membrane weight method [18].

$$\varepsilon = \frac{M_w - M_d}{\rho_w A l} \times 100\% \quad (1)$$

where M_W and M_d are the wet and dry membrane weight (g), respectively, A is the membrane area (cm^2), l is the average thickness (cm), and ρ_w is the density of water ($g\,cm^{-3}$).

Flow rate method was used to determine membrane pore size [19].

$$r_m = \sqrt{\frac{(2.9 - 1.75\varepsilon)\ 8\eta l Q}{\varepsilon A \Delta P}} \quad (2)$$

where ε is the porosity, η is the viscosity of water (Pa s), l is the membrane average thickness (cm), ΔP is the transmembrane pressure (MPa), A is the effective membrane area (cm^2), and Q is the volume of permeate pure water per unit time ($L\,h^{-1}$).

The first bubble pressure (FBP) and average bubble pressure (ABP) of membrane were measured by automatic filter integrity tester (FJLGUARD-311) using ethanol as medium [20].

Mechanical strength: Membrane mechanical strength was measured by Electronic yarn strength (HD021NS). The samples had the width of 1 cm and length of 15 cm. The folder distance was 100 mm and the tensile speed was $100\,mm\,min^{-1}$.

2.4. Filtration experiment

The water permeability and antifouling performance of membranes were evaluated in a dead-end stirred cell filtration system. The schematic diagram of the filtration experimental apparatus by using the flat membranes is shown in Fig. 1. In all experiments, constant agitation at the rate of 400 rpm was maintained and distilled water was used to characterize the pure water flux of the membranes. The membranes were pre-compressed with pure water at 0.15 MPa for 30 min with an effective area of 45.3 cm^2. Then, the pure water flux was determined at 0.1 MPa and the secondary effluent permeation was evaluated at 0.1 MPa for 5 h. All experiments were conducted at room temperature (25 ± 1°C). The pure water flux was calculated by Eq. (3):

$$J_w = \frac{Q}{A \Delta T} \quad (3)$$

where J_w is the pure water flux ($L\,m^{-2}\,h^{-1}$), Q is the volume of permeated water (L), A is the effective membrane area (m^2), and ΔT is the permeation time (h).

The rejection ratio (R_{BSA}) for BSA was calculated by the following equation:

$$R_{BSA}(\%) = \left(1 - \frac{2C_p}{C_f + C_r}\right) \times 100 \quad (4)$$

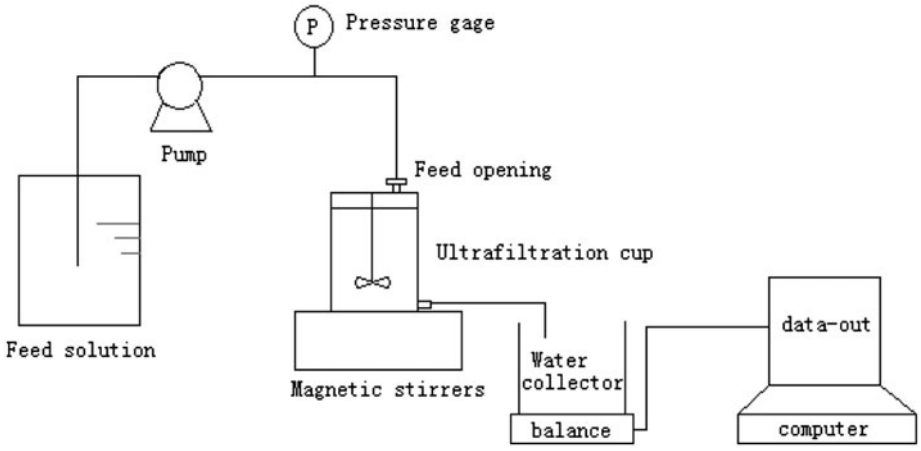

Fig. 1. Dead-end stirred cell filtration system.

where C_p, C_f, and C_r are the concentration in the permeate, the feed, and the remaining solution in mg L^{-1}, respectively. All feed concentrations were measured with a UV–vis spectrophotometer (UV-2100, UNIC) at a wave length of 280 nm [21].

2.5. Fouling index analysis

The relative flux used in this investigation is defined as the stabilized flux of secondary effluent divided by the pure water flux [21]. The relative flux was calculated by the following equation:

$$RF = \frac{J_p}{J_{w1}} \tag{5}$$

where RF is the relative flux, J_{w1} is the pure water flux (L m^{-2} h^{-1}), and J_p is the sewage flux (L m^{-2} h^{-1}).

The fouling degree of membranes was studied by fouling index which includes reversible fouling index (r_r) and irreversible fouling index (r_{ir}). Fouling process was performed according to ultrafiltration of feed at 0.1 MPa for 5 h. The fouling index was calculated by the following Eq.

$$r_r = \frac{J_{w2} - J_p}{J_{w1}} \tag{6}$$

$$r_{ir} = \frac{J_{w1} - J_{w2}}{J_{w1}} \tag{7}$$

where J_{w1} is the pure water flux (L m^{-2} h^{-1}), J_p is the sewage flux (L m^{-2} h^{-1}), J_{w2} is the pure water flux after physical cleaning [22,23] which includes water washing, backwashing, and wiping with absorbent cotton (L m^{-2} h^{-1}).

2.6. Membrane fouling evaluation

For information about the fouling evaluation of membrane, see references literature [24–26]. Fouling process was performed according to filter feed at 0.1 MPa for 5 h.

Fouling can be quantified by the resistance appearing during filtration [27]. The resistance is formed due to the formation of cake or gel layer on membrane surface. The flux (J), through the cake and membrane, may be described by Darcy's law:

$$J = \frac{\Delta P}{\mu \Sigma R} \tag{8}$$

where ΔP is the transmembrane pressure (MPa), μ is the viscosity of feed liquid (Pa s), and ΣR or (R_t) is the sum of the resistances. The intrinsic membrane resistance (R_m) can be estimated from initial pure water flux:

$$R_m = \frac{\Delta P}{\mu J_{w1}} \tag{9}$$

Fouling resistance (R_f) caused by pore plugging and irreversible adsorption of foulants on membrane pore wall and surface are calculated as following:

$$R_f = \frac{\Delta P}{\mu J_{ww}} - R_m \tag{10}$$

where J_{ww} is the pure water flux of fouled membrane.

Cake layer resistance (R_c) [28] formed on membrane surface can be calculated from the water flux after physical cleaning which includes water washing, backwashing, and wiping the surface with clean absorbent cotton:

$$R_c = \frac{\Delta P}{\mu J_p} - R_m - R_f \tag{11}$$

where J_p is the sewage flux. Concentration polarization resistance (R_p) formed by feed concentration on the membrane surface can be calculated from the water flux (J_p) after feed liquid filtration:

$$R_p = R_t - \frac{\Delta p}{\mu J_p} \tag{12}$$

The total filtration resistance (R_t) is the sum of R_m, R_p, R_f, and R_c.

In order to evaluate the fouling resistant ability of membranes, flux recovery ratio (FR) was introduced and calculated by Eq. (4):

$$FR = \frac{J_{w2}}{J_{w1}} \times 100\% \tag{13}$$

where J_{w1} is the pure water flux ($L\,m^{-2}\,h^{-1}$), J_{w2} is the pure water flux of membranes after physical wash which includes water washing, backwashing, and wiping with absorbent cotton ($L\,m^{-2}\,h^{-1}$).

3. Results and discussion

3.1. Light transmittance

Fig. 2 is light transmittance kinetic curve of different membranes. It shows that PP, PG, and P membranes have no delay time. PP and PG membranes tend to form dense surface because of the instantaneous demixing, and internal macroporous structure of the two membranes is formed due to liquid–liquid phase separation. The presence of different degrees of delay phase separation process, which illustrates the slow exchange speed of solvent and non-solvent in PA and PM membranes, may make macrovoids and loose sub-layer structure coexist in membranes, and this feature of PA membrane is more obvious.

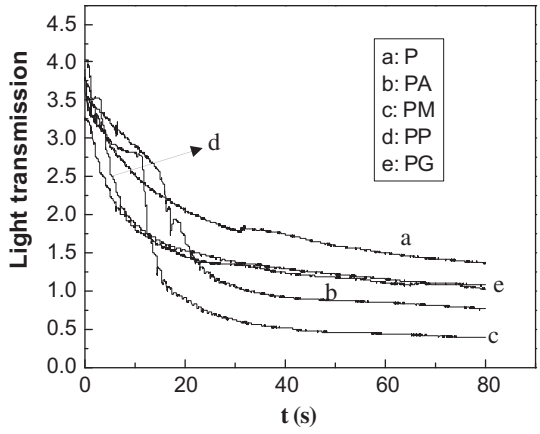

Fig. 2. Light transmission for precipitation of PVDF blend membranes in water.

3.2. Chemical composition of PVDF blend UF membranes

Fig. 3 is IR spectra of PVDF UF membranes, it can be found that the infrared spectrum of PG and PVDF membrane has no significant difference; C–O–C (ether bond) characterized absorption of PEG at 1,250 cm^{-1} does not exist in PG membrane, which illustrates that PEG has no residue in PG membrane substantially. While new absorption peaks at 3,370 cm^{-1} (hydroxyl in PVA), 1,728 cm^{-1} (ester carbonyl in PMMA), and 1,676 cm^{-1} (amide bond in PVP) appear in the IR spectrum of PA, PM, and PP blend membranes, respectively, which indicates that a certain amount of additives remain in blend membranes. The functional groups of the above polymers own certain polarity which helps them in forming hydrophilization effect on blend membranes.

3.3. Structure and morphology of blend membranes

Fig. 4 shows SEM images of surface and cross-section morphology of PVDF UF membranes. Arrows point to the top cortex of membranes. As can be seen from the figure that the cortex of pure PVDF membrane is thick and there are only a few dead-end pores under the cortex, the cross-section is dense but membrane surface exists crack pores. The surface of PA and PP membranes is smooth and dense, macrovoids in cross-section are through, and the cortex is thin. The support layer of PA membrane is loose sponge structure while the dense is the sub-layer of PP membrane. Not through teardrop-shaped pores distribute in the cross-section of PM and PG membranes whose surface is porous, and pores on the surface of PM membrane are large and intensive.

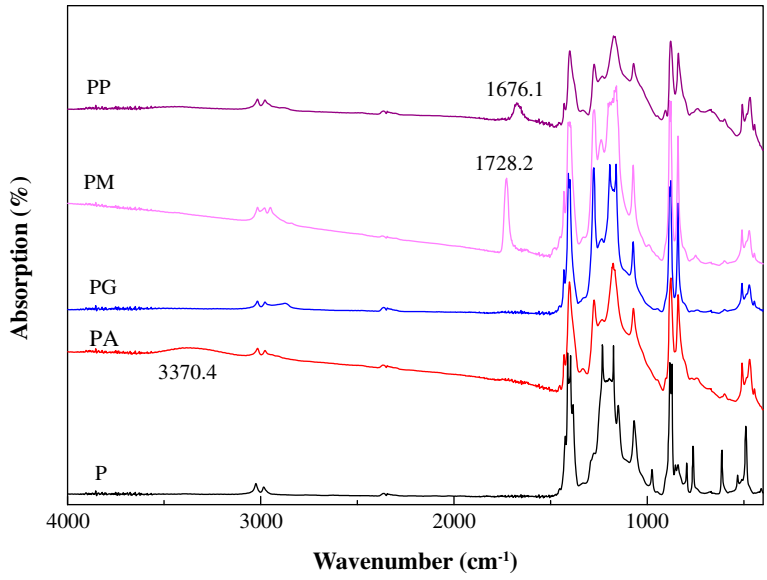

Fig. 3. FTIR spectra of PVDF UF membranes.

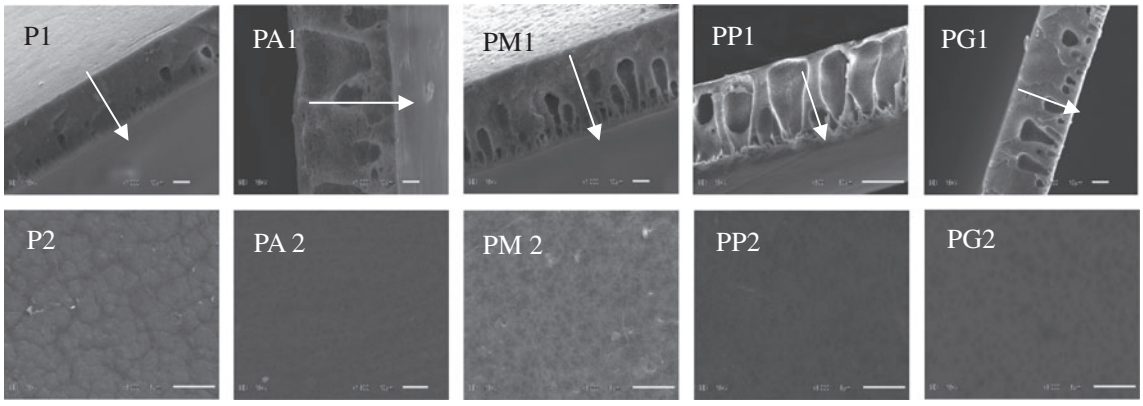

Fig. 4. SEM image of PVDF UF membrane (1: cross-section; 2: top surface; ×1,000).

Fig. 5 shows AFM images of PVDF UF membranes and the surface roughness of blend membranes is larger than that of pure PVDF membrane. Tiny concave–convex tissue distributes evenly on surface of PA membrane and PM membrane surface which result from delay in mixing. Obvious bag-like protuberance spread all over on the surface of PP and PG membranes and the average roughness of the two membranes is great, which is caused by instantaneous demixing.

3.4. Structure and performance parameter of PVDF blend membranes

Membrane structure and related performance parameters are listed in Table 2. The data show that when compared to P membrane, the FBP and ABP of blend membranes decline and the porosity and pore diameter are increased. WCA of modified membranes decreases, and the pure water flux of all blend membranes increases. Generally, the membranes with high surface roughness observed high flux and smooth surface exhibited lower flux and the contact angle of hydrophilic surface decreases with the increase in roughness. But in this study, one possible reason for the increase in flux is that the addition of polymer greatly improved membrane performance due to its hydrophilicity and high porosity structure [29–31]. The performance of PA and PP membrane changes more prominently. The hydrophilicity of PM and PG membranes is not high and the strength is declined. The ABP is similar to P membranes due to the alike

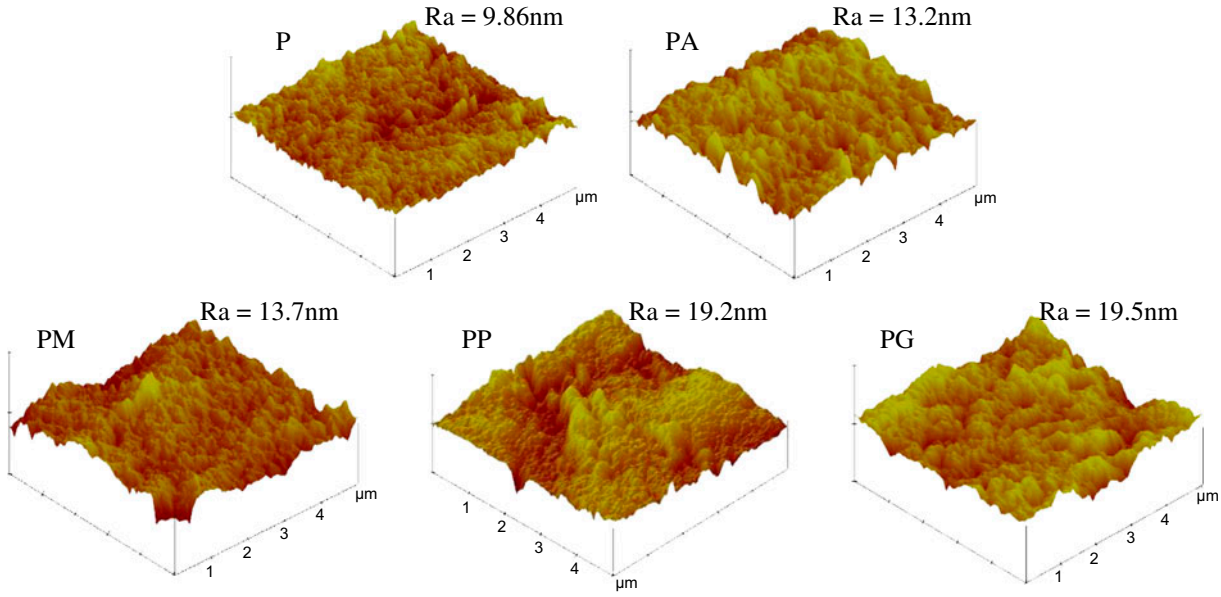

Fig. 5. AFM images of PVDF blend UF membranes.

Table 2
Properties of blend UF membranes

Membrane	ε (%)	r_m (nm)	FBP (kPa)	ABP (kPa)	S (MPa)	WCA (°)	J (L m^{-2} h^{-1})	R_{BSA} (%)
P	68.71	9.40	155.6	379.64	5.22	85.22	36.33	99.21
PA	80.24	26.91	52.71	190.13	3.02	56.80	217.5	78.20
PM	75.73	14.70	94.54	300.36	4.32	79.11	68.54	95.42
PP	86.53	18.29	86.22	206.21	4.09	65.32	255.6	95.52
PG	77.07	18.59	151.8	370.20	2.90	80.67	135.2	96.84

low porosity and dense section structure. The pure water flux and BSA retention rate are high especially for PG membranes which may be due to the rougher surface. These illustrate that PEG and PMMA failed to improve the hydrophilicity of PVDF membranes significantly, but they have certain impact on the structure and performance of PVDF membranes.

3.5. Membrane fouling of PVDF blend membranes

Table 3 shows the relative flux, fouling index, and cleaning recovery rate of PVDF UF membranes. As can be seen from Table 3, relative flux of blend membrane is close to that of P membrane except PM membrane. The cleaning recovery rate of PA and PP membrane is 100% and the irreversible fouling index r_{ir} is 0. The fouling index of PG membrane is high, irreversible fouling is more, and the cleaning recovery rate is only 55%. The fouling degree of PM membrane is high, the irreversible fouling is less, and the cleaning recovery rate is close to P membrane. From the membrane properties and structure parameters given in Table 2 and structural features shown in Fig. 1, it can be considered that PA and PP membranes with higher hydrophilicity could cause formation of a water molecule layer on the PVDF membrane surface and retard the hydrophobic foulants [32]. Also, PA and PP membrane internal macrovoids are through and the surface is dense, foulants in secondary effluent are not easy to enter and deposit on membrane surface because of the hydration layer.

Table 3
Fouling of secondary effluent on PVDF UF membranes

Membrane	RF	r_r	r_{ir}	FR (%)
P	0.78	0.31	0.17	92.12
PA	0.70	0.54	0	100.0
PM	0.30	0.35	0.12	88.32
PP	0.97	0.19	0	100.0
PG	0.65	0.21	0.45	55.21

So, PA and PP membranes are difficult to be fouled by secondary effluent and membrane fouling behavior is reversible. Because of the poor hydrophilicity, the porous surface, and the not through internal pores in PG and PM membranes, foulants can enter and deposit on membrane pore wall, causing irreversible fouling. So PG and PM membranes are easy to be fouled by secondary effluent and membrane fouling is irreversible.

3.6. Membranes fouling analysis

Fig. 6 is the fouling resistance analysis of effluent on blended PVDF UF membranes. Studying the nature of secondary effluent used in our experiment, it can be found that P, PM, and PG membranes with poor hydrophilicity and porous surface have great intrinsic membrane resistance, and hydrophobic organic foulants in secondary effluent can deposit on them easily. Also, the foulants with low molecular weight in sewage are easy to deposit on the membrane because it can flow easily through pores in PM and PG membranes. Therefore, P, PM, and PG membranes not only have higher concentration polarization and cake layer resistance but also have higher pore blocking resistance, resulting in irreversible membrane fouling behavior, so the antifouling is poor. The ordered hydration layer is formed on PA membrane surface due to strong hydrophilicity of PVA, causing the rapid increase in concentration polarization during initial stage of filtration. Nevertheless, the concentration polarization can be easily removed by hydraulic cleaning, and this is consistent with the high flux recovery rate of PA membranes. Foulants are not easy to accumulate in PA membranes with through macrovoids, causing pore plugging resistance and irreversible fouling; thus, PA membranes show better antifouling performance. While PP membrane surface is dense and it has litter intrinsic resistance due to the higher roughness and hydrophilicity which is consistent with the study results of Jeshi and Neville [12], also, the hydrophilicity PP membrane of can effectively prevent

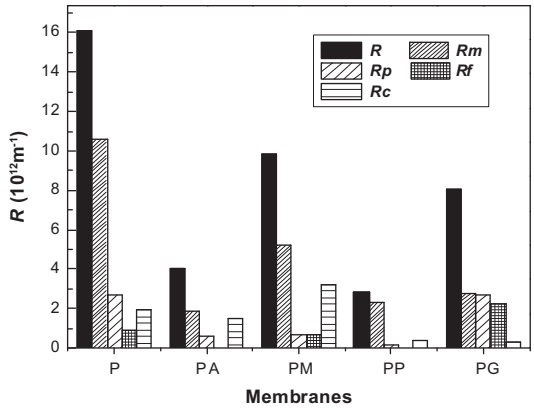

Fig. 6. Fouling resistance of PVDF UF membranes to secondary effluent.

foulants from entering. Moreover, the through macrovoids in membrane are not easy to preserve low molecular weight foulants which can cause pore plugging; therefore, the antifouling property of PP membranes is also excellent.

3.7. Treated water quality evaluations

Table 4 shows the water quality parameters of wastewater after being treated by PVDF blend UF membranes. The treated water quality for each membrane tested was obviously improved when compared with the raw water in Table 1. The data show the parameters of sewage which decreased more notably after being processed by P, PM, and PG membranes, due to low porosity, small pore size, and the serious pore blocking during ultrafiltration process of these membranes that remain favorable to reject macromolecular foulants. Part of the foulants can permeate membranes with big pore size and small cake layer and pore blocking resistance. Thus, the treated water quality of PA and PP membranes is slightly poorer than that of P, PM, and PG membranes, but it has reached the standard of reuse water. The increase of

Table 4
Results of treated water quality for each membrane tested

Membrane	SS (mg L^{-1})	COD (mg L^{-1})	TOC (mg L^{-1})	pH	Turbidity (NTU)	Molecular weight distribution (%)		
						<30 kDa	30–50 kDa	>50 kDa
P	0.5–1.0	1.8–2.3	1.5–1.9	6–7	0.3–0.6	83.1	15.1	1.8
PA	2.3–3.0	3.5–4.2	2.1–2.4	6–7	1.0–1.2	85.3	14.1	4.6
PM	1.1–2.0	2.3–2.7	1.7–2.3	6–7	0.8–1.1	83.1	14.4	2.5
PP	2.1–2.6	2.6–3.1	1.9–2.2	6–7	0.9–1.1	83.7	14.2	2.1
PG	1.0–1.5	2.0–2.4	1.6–2.0	6–7	0.8–1.0	83.1	14.9	2.0

the treated water pH may be due to the removal of the organics containing carboxyl (–COOH).

4. Conclusions

The antifouling evaluation of PVDF UF membranes prepared by blending with different polymers present in secondary effluent of urban sewage was studied and its conclusions are as following:

(1) Blending PEG and PMMA fails to improve the hydrophilicity of PVDF ultrafiltration membrane significantly. PG and PM membranes are easy to be fouled by secondary effluent due to their poor hydrophilicity, porous surface, and not through internal macrovoids. The irreversible fouling is caused by the severe pore plugging resistance especially for PG membrane. The surface properties of membrane such as roughness and hydrophilicity are the two key factors for the determination of the fouling behavior, and the hydrophilicity plays dominant role.

(2) PVDF UF membranes prepared by blending PVA have high hydrophilicity, dense surface, and through internal macrovoids; also, the sub-layer structure is loose. The flux of secondary effluent is high due to the strong hydrophilicity and smoother surface which has been proved by Zhao et al. [10]; the concentration polarization and filter cake layer resistance formed by foulants remain only on membrane surface. The fouling behavior on PA membrane is reversible, cleaning recovery rate is high, and the antifouling properties are better.

(3) Foulants are not easy to deposit on PP membrane due to its higher hydrophilicity, dense membrane surface, and support layer, also through internal macrovoids. The fouling resistance of secondary effluent on PP membrane is small, the water production rate is high, and it owns good antifouling property because of the dominant role of hydrophilicity though PP membrane has high roughness.

(4) The fouling analysis of the membranes revealed that surface hydrophilicity, structure, and roughness all have effect on antifouling ability of membranes. A pure water layer is easily formed on membrane surface with high hydrophilicity which can effectively prevent the adsorption and deposition of hydrophobic foulants onto membrane surface and reduce fouling. Foulants are not easy to deposit on membranes with high hydrophilicity and dense surface, also through internal macropores which are advantageous for the antifouling of membranes.

Acknowledgments

This research was financially supported by the National Natural Science Foundation of China (Grant Nos. 51008243, 51178378, 51278408), the Shaanxi Province Science and Technology research project (Grant No. 2013K13-01-03), and the Shaanxi Province Science and Technology innovation project (Grant Nos. 2012KTCL03-06, 2013KTCL03-16).

References

[1] Y.M. Kim, S.J. Kim, Y.S. Kim, S. Lee, I.S. Kim, J.H. Kim, Overview of systems engineering approaches for a large scale seawater desalination plant with a reverse osmosis network, Desalination 238 (2009) 312–332.
[2] A.D. Khawaji, I.K. Kutubkhanah, J.M. Wie, Advances in seawater desalination technologies, Desalination 221 (2008) 47–69.
[3] S. Wongchitphimon, R. Wang, R. Jiraratananon, L. Shi, C.H. Loh, Effect of polyethylene glycol (PEG) as an additive on the fabrication of polyvinylidene fluoride-co-hexafluropropylene (PVDF-HFP) asymmetric microporous hollow fiber membranes, J. Membr. Sci. 369 (2011) 329–338.
[4] J. Jiang, L. Zhu, L. Zhu, B. Zhu, Y. Xu, Surface characteristics of a self-polymerized dopamine coating deposited on hydrophobic polymer films, Langmuir 27 (2011) 14180–14187.
[5] S. Simone, A. Figoli, A. Criscuoli, M.C. Carnevale, A. Rosselli, E. Drioli, Preparation of hollow fibre membranes from PVDF/PVP blends and their application in VMD, J. Membr. Sci. 364 (2010) 219–232.
[6] Y. Chang, Y.-J. Shih, C.-Y. Ko, J.-F. Jhong, Y.-L. Liu, T.-C. Wei, Hemocompatibility of poly(vinylidene fluoride) membrane grafted with network-like and brush-like antifouling layer controlled via plasma-induced surface PEGylation, Langmuir 27 (2011) 5445–5455.
[7] S.J. Oh, N. Kim, Y.T. Lee, Preparation and characterization of PVDF/TiO_2 organic–inorganic composite membranes for fouling resistance improvement, J. Membr. Sci. 345 (2009) 13–20.
[8] H. Susanto, M. Ulbricht, Characteristics, performance and stability of polyethersulfone ultrafiltration membranes prepared by phase separation method using different macromolecular additives, J. Membr. Sci. 327 (2009) 125–135.
[9] H.P. Srivastava, G. Arthanareeswaran, N. Anantharaman, V.M. Starov, Performance of modified poly(vinylidene fluoride) membrane for textile wastewater ultrafiltration, Desalination 282 (2011) 87–94.
[10] C. Zhao, X. Xu, J. Chen, F. Yang, Effect of graphene oxide concentration on the morphologies and antifouling properties of PVDF ultrafiltration membranes, J. Environ. Chem. Eng. 1 (2013) 349–354.

[11] P. Wang, Z. Wang, Z. Wu, S. Mai, Fouling behaviours of two membranes in a submerged membrane bioreactor for municipal wastewater treatment, J. Membr. Sci. 382 (2011) 60–69.
[12] S.A. Jeshi, A. Neville, An investigation into the relationship between flux and roughness on RO membranes using scanning probe microscopy, Desalination 189 (2006) 221–228.
[13] M. Hashino, T. Katagiri, N. Kubota, Y. Ohmukai, T. Maruyama, H. Matsuyama, Effect of surface roughness of hollow fiber membranes with gear-shaped structure on membrane fouling by sodium alginate, J. Membr. Sci. 366 (2011) 389–397.
[14] A. Rahimpour, S.S. Madaeni, M. Jahanshahi, Y. Mansourpanah, N. Mortazavian, Development of high performance nano-porous polyethersulfone ultrafiltration membranes with hydrophilic surface and superior antifouling properties, Appl. Surf. Sci. 255 (2009) 9166–9173.
[15] F. Wei, Monitoring and Analysis Method of Water and Wastewater, fourth ed., Beijing Environmental Science Press, China, 2002.
[16] E.M. Thurman, R.L. Malcolm, Preparative isolation of aquatic humic substances, Environ. Sci. Technol. 15 (1981) 463–466.
[17] A. Rahimpour, S.S. Madaeni, Y. Mansourpanah, Nano-porous polyethersulfone (PES) membranes modified by acrylic acid (AA) and 2-hydroxyethylmethacrylate (HEMA) as additives in the gelation media, J. Membr. Sci. 364 (2010) 380–388.
[18] Q.-Z. Zheng, P. Wang, Y.-N. Yang, D.-J. Cui, The relationship between porosity and kinetics parameter of membrane formation in PSF ultrafiltration membrane, J. Membr. Sci. 286 (2006) 7–11.
[19] C. Feng, B. Shi, G. Li, Y. Wu, Preparation and properties of microporous membrane from poly(vinylidene fluoride-co-tetrafluoroethylene) (F2.4) for membrane distillation, J. Membr. Sci. 237 (2004) 15–24.
[20] A. Hernández, J.I. Calvo, P. Prádanos, F. Tejerina, Pore size distributions in microporous membranes. A critical analysis of the bubble point extended method, J. Membr. Sci. 112 (1996) 1–12.
[21] L. Wu, J. Sun, Q. Wang, Poly(vinylidene fluoride)/polyethersulfone blend membranes: Effects of solvent sort, polyethersulfone and polyvinylpyrrolidone concentration on their properties and morphology, J. Membr. Sci. 285 (2006) 290–298.
[22] M. Mänttäri, L. Puro, J. Nuortila-Jokinen, M. Nyström, Fouling effects of polysaccharides and humic acid in nanofiltration, J. Membr. Sci. 165 (2000) 1–17.
[23] S. Liang, K. Xiao, Y. Mo, X. Huang, A novel ZnO nanoparticle blended polyvinylidene fluoride membrane for anti-irreversible fouling, J. Membr. Sci. 394–395 (2012) 184–192.
[24] N. Maximous, G. Nakhla, W. Wan, K. Wong, Preparation, characterization and performance of Al_2O_3/PES membrane for wastewater filtration, J. Membr. Sci. 341 (2009) 67–75.
[25] A. Rahimpour, M. Jahanshahi, N. Mortazavian, S.S. Madaeni, Y. Mansourpanah, Preparation and characterization of asymmetric polyethersulfone and thin-film composite polyamide nanofiltration membranes for water softening, Appl. Surf. Sci. 256 (2010) 1657–1663.
[26] T. Wang, Y.-Q. Wang, Y.-L. Su, Z.-Y. Jiang, Antifouling ultrafiltration membrane composed of polyethersulfone and sulfobetaine copolymer, J. Membr. Sci. 280 (2006) 343–350.
[27] S.S. Madaeni, Y. Mansourpanah, Chemical cleaning of reverse osmosis membranes fouled by whey, Desalination 161 (2004) 13–24.
[28] S. Jamal Khan, C. Visvanathan, V. Jegatheesan, Prediction of membrane fouling in MBR systems using empirically estimated specific cake resistance, Bioresour. Technol. 100 (2009) 6133–6136.
[29] J.H. Xu, M. Li, Y. Zhao, Advance of wetting behavior research on the superhydrophobic surface with micro- and nano-structures, Prog. Chem. 18(11) (2006) 1425–1433 (in Chinese).
[30] P. Gomez-Romero, Hybrid organic–inorganic materials—in search of synergic activity, Adv. Mater. 13 (2001) 163–174.
[31] S.B. Teli, S. Molina, E.G. Calvo, A.E. Lozano, J. de Abajo, Preparation, characterization and antifouling property of polyethersulfone-PANI/PMA ultrafiltration membranes, Desalination 299 (2012) 113–122.
[32] G.-d. Kang, Y.-m. Cao, Development of antifouling reverse osmosis membranes for water treatment: A review, Water Res. 46 (2012) 584–600.